INNOVATIVE DESIGN OF A DUAL WIDEBAND 2×2 MIMO ANTENNA FOR TERAHERTZ APPLICATIONS

BILAL AGHOUTANE[1]

Ibn Tofail University, Faculty of science, Kenitra, Morocco

HANAN EL FAYLALI

Ibn Tofail University, Faculty of science, Kenitra, Morocco

The article presents design and steps involved in designing a wideband multiband optimized MIMO antenna for terahertz (THz) applications. The 2x2 MIMO antenna is designed by incorporating combinations of circular and rectangular shaped slots, and the ground plane is modified with an extended circular shaped defect. The bandwidth of the proposed antenna is improved by altering full ground to partial ground. The dual band 2x2 MIMO antenna provides (26.66% 1.3-1.7THz) and (51.66% 3.9-7THz) impedance bandwidth achieving <−25 dB isolation between the antenna elements and having a peak gain of 8.8dB. In addition, it has an omnidirectional radiation character with high-directivity that allow the transmitter signal to be propagated over a practical communication channel. Moreover, the feature is evaluated by computing MIMO metric parameters such as Diversity Gain (DG), Envelope Correlation Coefficient (ECC), Mean Effective Gain (MEG), Total Active Reflection Coefficient (TARC) and Channel Capacity Loss (CCL). The proposed 2x2 MIMO antenna could be an excellent candidate for high-speed indoor wireless communication systems as well as for explosive detections, homeland defense system, medical imaging, pharmaceutical analysis and material characterization application.

Keywords: MIMO antenna, THz applications, wireless systems.

1. Introduction

The use of electromagnetic waves in the terahertz frequency range (100 GHz - 20 THz) has long been hampered on the one hand by the difficulty in developing sufficiently powerful THz radiation sources, and on the other hand by the lack of easy-to-use detectors [1]. Moreover, propagation losses is another challenging task in terahertz band [2]. Indeed, Since the 1990s, there has been a real technological revolution in this field and very significant progress has been made in the generation and detection of terahertz (THz) waves [3]. Thus, one begins to find in laboratories THz sources operating in pulsed (of the order of µW) or continuous (of the order of mW) with reasonable output powers. In parallel, we see the appearance of the first THz matrix detectors. If the performance levels achieved today with these components seem insufficient, it seems clear that technological developments will allow in the relatively near future to achieve performance allowing to consider the marketing of systems using THz technology. Currently, the situation is changing, with the emergence of applications such as broadband telecommunications, medical imaging and biology [4, 5]. In these applications, the presence of a terahertz

antenna is essential. Working on THz antenna while preserving the low profile feature continues to be very challenging.

Among various terahertz antennas, a microstrip patch antenna has been widely used since it is cost effective, light weight, and easy to design and fabrication [6]. In this direction, many works have been carried out to propose appropriates antennas for THz application [7-13]. In [7], a circular patch with triangular shaped substrate is proposed. The impedance matching of the proposed antenna is 371GHz with a peak gain of 6.33 dB. A VSWR (voltage standing wave ratio) less than 1.005 is obtained at operating band. Cheng et al. propose in [8], a terahertz patch antenna. The antenna offers a peak gain of 7.79 dB with a bandwidth of 0.04 THz. These performances are obtained by coating an epsilon-near-zero (ENZ) metamaterial superstrate. In [9] the performance of a frequency reconfigurable THz microstrip slot antenna is evaluated. The antenna works from 2.8 to 4.2 THz by offering a gain of about 2dB. Shalini et al. [10] have introduce a compact circular polarized patch antenna for THz applications. An impedance matching of 0.5 THz at 2.05 is realized. The introduced antenna with a VSWR less than 1.5, has a peak gain of 5.02 dB. In [11] a slotted tube antenna structure is analyzed in the THz band. The antenna with a return loss of −57.81 dB offering a bandwidth of 0.052 and has a VSWR of 1.002. A U-shaped slot printed antennas is proposed in [12] for THz applications. the antenna bandwidth ranges from 0.68 to 1.63 THz with a directivity of 6.60 dB. The VSWR value of the proposed antenna is 1.007. In [13] the performance of a circular patch antenna for terahertz applications is analyzed. The designed antenna with a VSWR of 1.0003 offers an impedance bandwidth of 0.386 THz at 7 THz and has a peak gain of 7.286 dB.

. **Table 1.** The performance proposed MIMO antenna versus other MIMO antennas from literature.

Reference	Directivity (dB)	Gain (dB)	Bandwidth (THz)	Return loss (dB)	Resonance frequency (THz)
[7] Khan (2020)	7,91	5.15	0.677	-48.85	-
[8] Cheng (2020)	-	7.79	0.04	-	-
[9] Khatereh (2021)	-	2	1.4	-	-
[10] Shalini (2021)	-	5.02	0.5	-	2.05
[11] Britto (2021)	7.68	9.2	0.052	−57.81	2.37
[12] Shamim (2021)	6.60	-	0.53 - 0.84	-	-
[13] Khan (2020)	7.4	7.2	0.386	-	-
This work	10.38	8.8	(1.3-1.7) & (3.9-7)	-18 & -24	1.5 & 6.0

On our we side, the antenna is designed by incorporating combinations of circular and rectangular shaped slots, and the ground plane is modified with an extended circular shaped defect. The final single element is designed in four steps starting with a simple rectangular as a patch and by adding four slots and a circle in the patch. Based on this single element,

we designed a 2x2 MIMO technique. MIMO system is used in this work because it can increase significantly the throughput without additional bandwidth and extends the radio coverage without increasing the transmission power [14]. The proposed antenna is working efficiently over a frequency spectrum of 1.3-1.7 THz and 3.9-7.0 THz with a peak gain of 8.8 dBi at 6 THz a long with desirable radiation patterns. Moreover, the antenna has a compact size compared to the early described structures. Consequently, the 2x2 MIMO antenna can be used efficiently for different terahertz (THz) applications such as high-speed indoor communications, detection, pharmaceutical analysis and material characterization application, explosive detections etc.

2. Proposed reconfigurable antenna

The intermediate steps of the derivation of the MIMO element are presented in Fig. 2. The single element design started with a microstrip rectangular patch loaded with four rectangular slots and a circular slot at the center. These slots help distribute the surface current at the circumference of a rectangular antenna with negligible current concentration at the edge. Based on the same element, we derived the 2 ports MIMO antenna. The same basic element is used to design the proposed 2x2 MIMO antenna as shown in figure 2. The corporate feed waveguide is implemented by using the techniques of ground plane extension and the addition of lumped port between the feedline and ground plane. The optimized dimensions of the proposed antenna are depicted in table 2. The proposed 2x2 MIMO antenna designed on a 0.5 μm Rogers RT/duriod 6010 substrate size of $47.916 \times 37.693\ \mu m^2$ with relative dielectric permittivity equal 10.2 and tangent loss 0.0023 to operate on Terahertz.

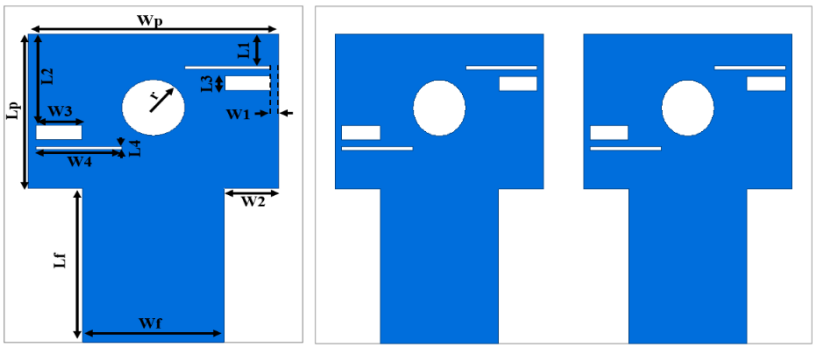

(a) ***(b)***

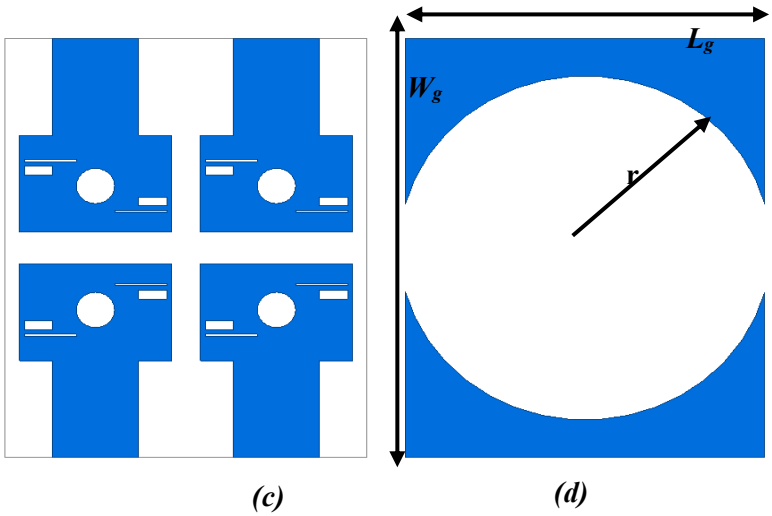

Figure 1. antennas geometries: (a) single element, (b) two port MIMO antenna, (c) 2x2 MIMO Top view, (d) 2x2 MIMO Bottom view. With $d' = 7.168$ µm & $r = 39$ µm.

Table 2. The optimized dimensions of the proposed antenna

Parameters	Dimensions (μm)	Parameters	Dimensions (μm)
W_p	31.693	W_2	6.92325
L_p	21.958	L_2	12.979
W_f	17.8465	W_3	5.8465
L_f	21.958	L_3	2
W_g	37.693	W_4	10.8465
L_g	47.916	L_4	0.5
W_1	1	r	4
L_1	4.479		

3. Antenna Performance and discussions

3.1. *S-parameters and radiation patterns analysis*

A comparison between the three configurations cited above in terms of S11 is shown in figure 2. One can notice from figure 2 that the 2x2 MIMO performs better than the single and two ports MIMO antenna in terms of bandwidth and return loss. This is due that in 2x2 MIMO we defected the ground plane with a circular shaped slot. Thanks to its high performance, 2x2 MIMO antenna will be used in this work.

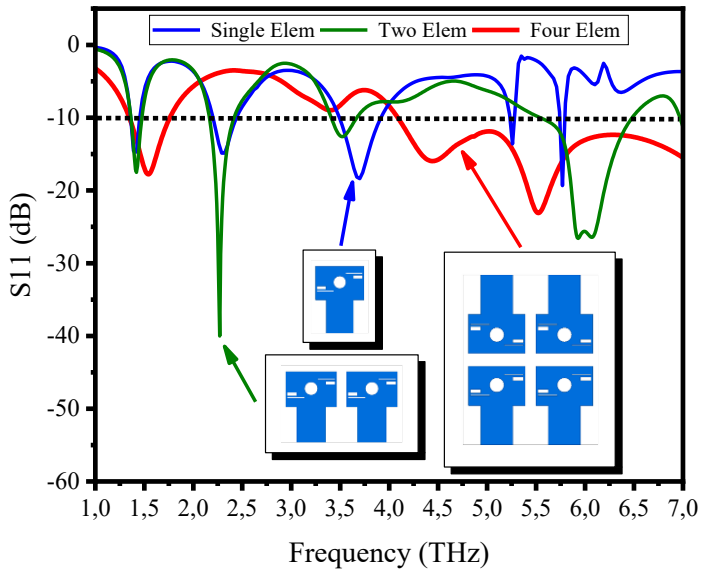

Figure 2. Comparison of S11 between single element, two-element, and MIMO antenna proposed for Terahertz.

To draw a clear picture of the proposed antenna, we simulate the reflection coefficient for each element of the 2x2 MIMO antenna as well as the isolation between antenna elements. Figure 3 (a) shows the S11, S22, S33, S44 for 2x2 MIMO antenna. It can be observed that the 2x2 MIMO antenna covers the 3.9-7 THz band. Similar reflection coefficient curves are obtained for different antenna elements with a slight shift in bands. Likewise, figure 3 shows the isolation of the proposed 2x2 MIMO antenna. To better understand the isolation between elements, we analyze the coupling between diagonal antennas, vertical antennas and horizontal antennas. The proposed antenna is also a dual-band antenna which means it gives more chance for more applications to be used in these two bands. The mutual coupling between diagonal antennas (1,4 and 2,3) is less than -25 dB in the whole band and is the lowest among the other cases. Coupling between vertical elements (1,3 and 4,2) is well below -25 dB and is the highest among the others one. These results can be explained by the distance inter-elements. Because the distance between the diagonal elements is the highest one, and it is the lowest one for the horizontal elements. Similar isolation between elements is obtained for each case (diagonal, horizontal and vertical elements) with a slight shift in some bands.

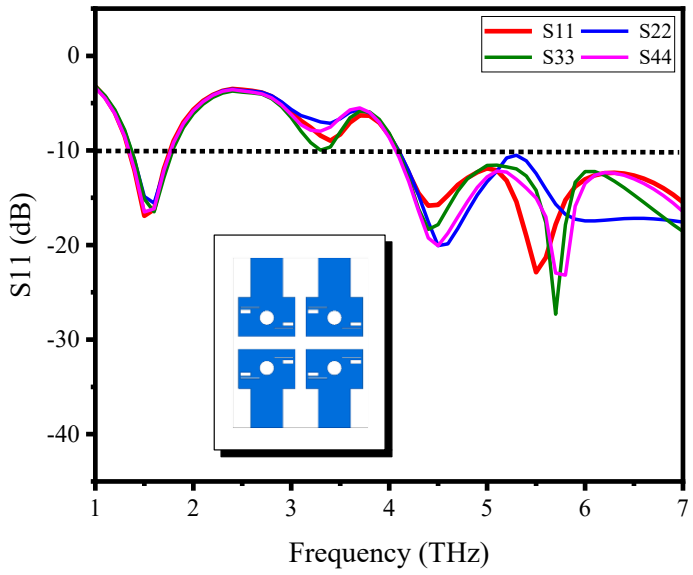

(a)

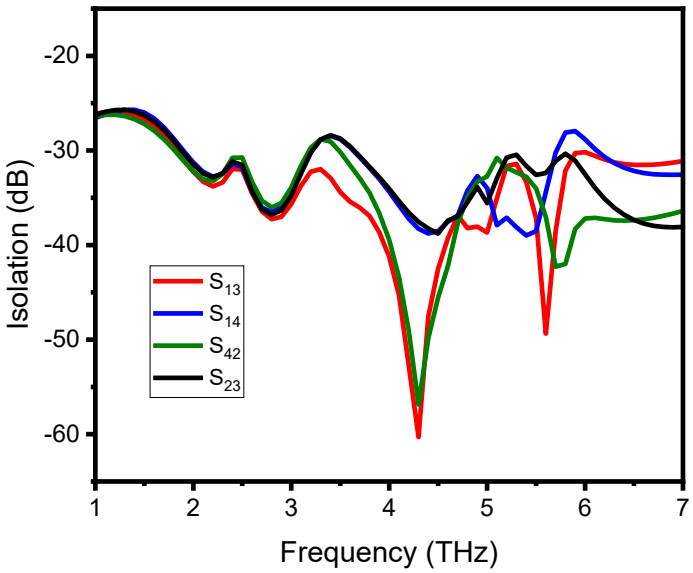

(b)

Figure 3. S-Parameters simulation of the proposed 2x2 MIMO antenna (a) reflection coefficient, (b) isolation.

Figure 4 shows the Normalized 2D radiation patterns at 4.5 THz of the 2x2 MIMO antenna. The patterns are represented in the E- and H-plane which correspond to yz- and xz- planes of the antenna orientation. Figure 5 displays that the E- and H- plane radiation pattern of the proposed antenna is directional at 4.5 THz. Moreover, it is observed that the E-plan and

H-plan patterns are almost identical with the main lobe at 105°. The obtained main lobe with a narrow beam leads to higher gain. Besides, the H-plane beam pattern is similar to the E-plane beam pattern at the air-dielectric interface.

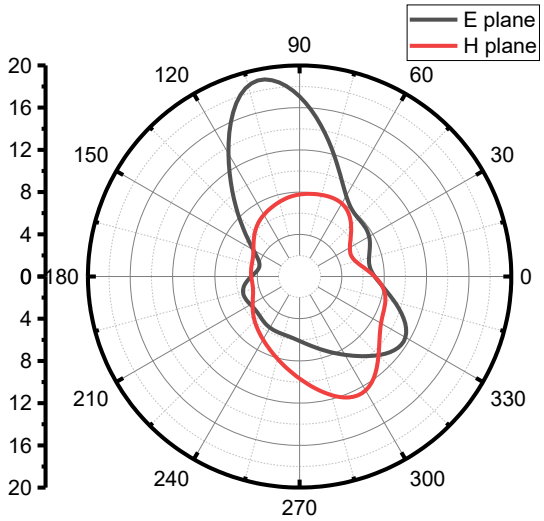

Figure 4. E-plane and H-plane of the MIMO antenna proposed for Terahertz.

3.2. *MIMO performance Diversity Analysis*

To validate the proposed MIMO antenna, we will evaluate the MIMO diversity parameters such as MEG, CCL, ECC, DG and TARC. These MIMO metrics parameters will allow us to draw a clear picture on antenna diversity and performance [15-18]. Firstly, we will evaluate the ECC and DG metrics. The following expression is used to calculate the Envelope Correlation Coefficient (ECC) the relations given bellow [17] :

$$\rho_{eij} = \frac{\left|\sum_{n=1}^{N} S_{i,n}{}^{*} S_{n,j}\right|^{2}}{\prod_{K=(i,j)}\left[1-\sum_{n=1}^{N} S_{k,n}{}^{*} S_{n,k}\right]} \quad (1)$$

Where i, j and N are the i[th] antenna, jth antenna and the total number of antenna respectively. based on the above expression we can calculate $ECC_{1,2}$, $ECC_{3,4}$, $ECC_{1,3}$ and $ECC_{1,4}$ which are given by:

$$ECC_{1,2} = \frac{|S_{11}{}^{*}S_{12} + S_{12}{}^{*}S_{22} + S_{13}{}^{*}S_{32} + S_{14}{}^{*}S_{42}|^{2}}{\left(1-(|S_{11}|^{2}+|S_{21}|^{2}+|S_{31}|^{2}+|S_{41}|^{2})\right)\left(1-(|S_{12}|^{2}+|S_{22}|^{2}+|S_{32}|^{2}+|S_{42}|^{2})\right)} \quad (2)$$

$$ECC_{3,4} = \frac{|S_{31}{}^{*}S_{14} + S_{32}{}^{*}S_{24} + S_{33}{}^{*}S_{34} + S_{34}{}^{*}S_{44}|^{2}}{\left(1-(|S_{13}|^{2}+|S_{23}|^{2}+|S_{33}|^{2}+|S_{43}|^{2})\right)\left(1-(|S_{14}|^{2}+|S_{24}|^{2}+|S_{34}|^{2}+|S_{44}|^{2})\right)} \quad (3)$$

$$ECC_{1,3} = \frac{|S_{11}{}^{*}S_{13} + S_{12}{}^{*}S_{23} + S_{13}{}^{*}S_{33} + S_{14}{}^{*}S_{43}|^2}{\left(1-(|S_{11}|^2+|S_{21}|^2+|S_{31}|^2+|S_{41}|^2)\right)\left(1-(|S_{13}|^2+|S_{23}|^2+|S_{33}|^2+|S_{43}|^2)\right)} \quad (4)$$

$$ECC_{1,4} = \frac{|S_{11}{}^{*}S_{14} + S_{12}{}^{*}S_{24} + S_{13}{}^{*}S_{34} + S_{14}{}^{*}S_{44}|^2}{\left(1-(|S_{11}|^2+|S_{21}|^2+|S_{31}|^2+|S_{41}|^2)\right)\left(1-(|S_{14}|^2+|S_{24}|^2+|S_{34}|^2+|S_{44}|^2)\right)} \quad (5)$$

Also, the diversity gain (DG) of the proposed antenna MIMO antenna can be computed using the relation given below:

$$DG = 10\sqrt{1-|\rho_{eij}|^2} \quad (6)$$

According to [15], the ECC and DG values should be less than 0.05 and greater than 9.95, respectively. Here, the proposed antenna offers an ECC value less than 0.001 and DG value greater than 9.99 at the operating bands, as shown in figure 5. So, the obtained results is within the desired value which indicates good radiation diversity performance.

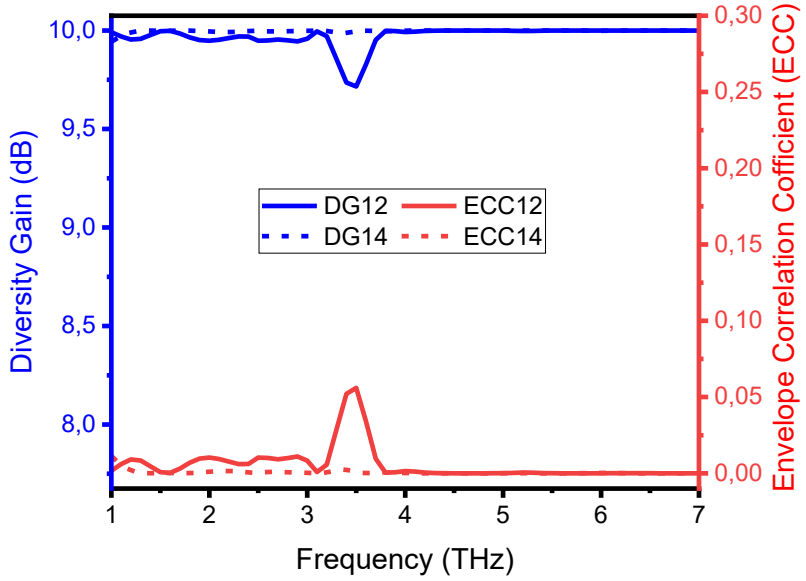

Figure 5. ECC and DG of the MIMO antenna proposed for Terahertz

The second parameter that we will evaluated is the TARC parameter. It is an essential parameter to define frequency bandwidth and radiation performance under the different nature of MIMO antennas. TARC parameter gives more detail about mutual coupling and signal combinations between ports [16]. The following expression can be used to calculate the TARC [18]:

$$TARC = \frac{\sqrt{\sum_{i=1}^{N}|S_{i1} + \sum_{m=2}^{N} S_{im}e^{j\theta_{m-1}}|}}{\sqrt{N}} \quad (7)$$

So, the TARC can be expressed as:

$$TARC = \frac{\sqrt{\begin{matrix}|S_{11}+S_{12}e^{j\theta_1}+S_{13}e^{j\theta_2}+S_{14}e^{j\theta_3}|^2 \\ +|S_{21}+S_{22}e^{j\theta_1}+S_{23}e^{j\theta_2}+S_{24}e^{j\theta_3}|^2 \\ +|S_{31}+S_{32}e^{j\theta_1}+S_{33}e^{j\theta_2}+S_{34}e^{j\theta_3}|^2 \\ +|S_{41}+S_{42}e^{j\theta_1}+S_{43}e^{j\theta_2}+S_{44}e^{j\theta_3}|^2\end{matrix}}}{\sqrt{4}} \quad (8)$$

Figure 6 shows the TARC value versus frequency for deferent angle value. As can be observed in figure 6, the TARC is less than -10dB at the operating bands which means that the mutual coupling between antenna decreases in the operating bands. So, the obtained TARC value indicates good matching, which confirms the results obtained for isolation (depicted in figure 3).

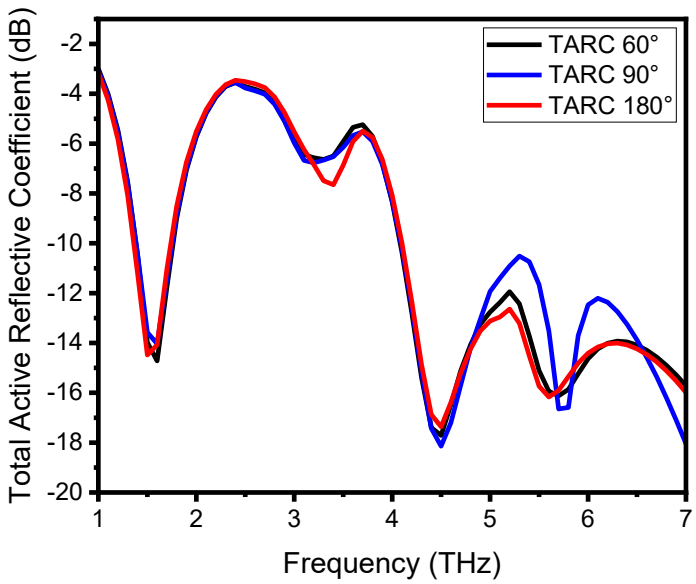

Figure 6. TARC of the MIMO antenna proposed for Terahertz

CCL parameter is another critical parameter which was also studied in this work. This parameter defines the capacity of a system that can be attained with less loss over the channel, approximately loss less than 0.4 bits/ s/Hz at the operating band [15]. Figure 7 depicted the CCL parameter as a function of frequency. As can be seeing from figure 7, the CCL value is less than 0.4 at the two operating bands. This result indicate that the proposed antenna can carry more data rate with less loss.

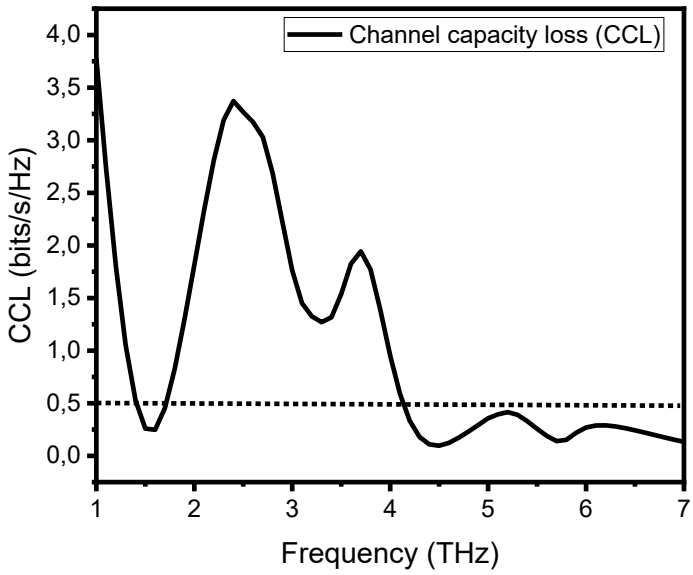

Figure 7. CCL of the MIMO antenna proposed for Terahertz

It can be computed using the following equation:

$$C_{loss} = -log_2\ det(\alpha^R) \tag{9}$$

$$\text{Where } \alpha^R = \begin{bmatrix} \alpha_{11}\alpha_{12}\alpha_{13}\alpha_{14} \\ \alpha_{21}\alpha_{22}\alpha_{23}\alpha_{24} \\ \alpha_{31}\alpha_{32}\alpha_{33}\alpha_{34} \\ \alpha_{41}\alpha_{42}\alpha_{43}\alpha_{44} \end{bmatrix} \tag{10}$$

Where $\alpha_{ii} = 1 - \left(\sum_{j=1}^{N} |S_{ij}|^2\right)$And $\alpha_{ij} = -\left(S_{ij}{}^* S_{ij} + S_{ji}{}^* S_{ij}\right)$

Another parameter (MEG) that quantifying the average strength of the path for each antenna element is also discussed. The MEG results show that the MEG value is between -4 and -3 dB at the two operating bands, as shown in figure 8, which is in good agreement with real-world standard (between -4 and -3 dB) for MEG value [16]. In the case of the Rayleigh environment, the MEG can be expressed as [18]:

$$MEG_i = 0.5 \left[1 - \sum_{j=1}^{N} |S_{ij}|^2\right] \tag{11}$$

Also

$$\left|MEG_i - MEG_j\right| < 3\ dB \tag{12}$$

Thus, the obtained results show better diversity performance which indicates that the proposed antenna works efficiently in the THz band.

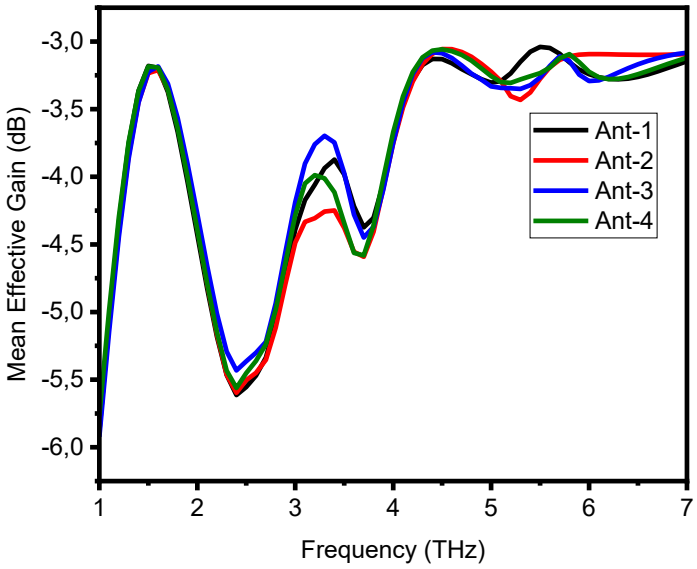

Figure 8. MEG of the MIMO antenna proposed for Terahertz

4. Conclusion

The design, analysis and simulation results of a dual wideband 2x2 MIMO antenna are presented in this article. The presented prototype antenna geometry gives rise to a wideband simulated, which is 213GHz (1.306-1.519THz), related to the first resonance frequency and 3.1THz (3.9-7THz) corresponding to the second resonance frequency. Moreover, the isolation is less than −25 dB between the antenna elements and having a peak gain of 8.8dBi. Finally, the prototype antenna covers the Terahertz band for THz application, and it may be helpful in explosive detections, homeland defense systems, medical imaging, pharmaceutical analysis and material characterization application.

Declaration

Data Availability All the data generated during and/or analyzed during the current study are available from the corresponding author on reasonable request.

Informed consent Informed Consent was obtained from all authors.

Consent for Publication The authors confirm that there is informed consent to the publication of the data contained in the article.

Conflict of Interest The authors declare that they have no conflict of interests.

Funding Not applicable.

Code Availability The paper deals with software application. The EM solver software HFSS is used for the design, simulation and data collection purposes

5. References

[1] Kim, S-M, Hong, S-M, Jang, J-H. Strong and narrowband terahertz radiation from GaAs based pHEMT and terahertz imaging. Microw Opt Technol Lett. 2020; 62: 3791– 3795. https://doi.org/10.1002/mop.32525

[2] Aghoutane, B., El Ghzaoui, M. & El Faylali, H. Spatial characterization of propagation channels for terahertz band. SN Appl. Sci. 2021; 3, 23. https://doi.org/10.1007/s42452-021-04262-8

[3] X. Ropagnol, M. Matoba, J. E. Nkeck, F. Blanchard, E. Isgandarov, J. Yumoto, and T. Ozaki "Efficient terahertz generation and detection in cadmium telluride using ultrafast ytterbium laser", Applied Physics Letters 2020; 117, 181101. https://doi.org/10.1063/5.0024112

[4] Kawanishi, T., Inagaki, K., Kanno, A., Yamamoto, N., Aiba, T., Yasuda, H., & Wakabayashi, T. (2021). Terahertz and photonics seamless short-distance links for future mobile networks. Radio Science 2020; 56, e2020RS007156. https://doi.org/10.1029/2020RS007156

[5] Qiao, H-D, Liu, H, Mou, J-C, Lv, X. "220 GHz focal plane imaging demonstration using integrated terahertz array detector" Microw Opt Technol Lett. 2020; 62: 2826– 2829. https://doi.org/10.1002/mop.32388

[6] Tang, X, Yu, B, Li, Y, Chen, H. A low-profile dual-polarized stacked patch antenna array with mutual coupling reduction for massive MIMO. Int J RF Microw Comput Aided Eng. 2021; e22713. https://doi.org/10.1002/mmce.22713

[7] Khan MAK, Shaem TA, Alim MA Graphene patch antennas with different substrate shapes and materials. Optik 2020; 202: 163700. https://doi.org/10.1016/j.ijleo.2019.163700

[8] Cheng, C., Lu, Y., Zhang, D., Ruan, F., & Li, G. ""Gain enhancement of terahertz patch antennas by coating epsilon-near-zero metamateials". Superlattices and Microstructures 2020; 139, 106390. https://doi:10.1016/j.spmi.2020.106390

[9] Khatereh Moradi, Ali Pourziad, Saeid Nikmehr, "A frequency reconfigurable microstrip antenna based on graphene in Terahertz Regime", Optik 2021; Volume 228, 166201. https://doi.org/10.1016/j.ijleo.2020.166201.

[10] Shalini M., Ganesh Madhan M., "A compact antenna structure for circular polarized terahertz radiation", Optik 2021; Volume 231, , 166393. https://doi.org/10.1016/j.ijleo.2021.166393.

[11] Britto, EC, Danasegaran, SK, Johnson, W. Design of slotted patch antenna based on photonic crystal for wireless communication. Int J Commun Syst. 2021; 34:e4662 https://doi.org/10.1002/dac.4662

[12] Shamim, S.M., Das, S., Hossain, M.A. et al. Investigations on Graphene-Based Ultra-Wideband (UWB) Microstrip Patch Antennas for Terahertz (THz) Applications. Plasmonics 2021. https://doi.org/10.1007/s11468-021-01423-8

[13] Khan, M.A.K., Ullah, M.I., Kabir, R. et al. High-Performance Graphene Patch Antenna with Superstrate Cover for Terahertz Band Application. Plasmonics 2020; 15, 1719–1727. https://doi.org/10.1007/s11468-020-01200-z

[14] Salman Khalid, Rashid Mehmood, Waqas Bin Abbas, Farhan Khalid, Muhammad Naeem, "Joint transmit antenna selection and precoding for millimeter wave massive MIMO systems," Physical Communication,Volume 42, 2020, 101137, https://doi.org/10.1016/j.phycom.2020.101137.

[15] Amit Kumar, Abdul Quaiyum Ansari, Binod Kumar Kanaujia, JugulKishor, (2019) "A novel ITI-shaped isolation structure placed between two-port CPW-fed dual-band MIMO

antenna for high isolation", AEU - International Journal of Electronics and Communications, Vol 104. https://doi.org/10.1016/j.aeue.2019.03.009.

[16] Ramachandran, A., Mathew, S., Viswanathan, V. P., Pezholil, M., & Kesavath, V. (2016). Diversity-based four-port multiple input multiple output antenna loaded with interdigital structure for high isolation. IET Microwaves, Antennas & Propagation, 10(15), 1633–1642. doi: https://doi.org/10.1049/iet-map.2015.0828

[17] Kompella S.L.ParvathiSudha R.Gupta (2021)"Novel dual-band EBG structure to reduce mutual coupling of air gap based MIMO antenna for 5G application", Int. J. Electron. Commun. (AEÜ) 138, 153902.

[18] CORREIA L. "COST 259 final report: wireless flexible personalised communications" (Wiley, 2001)